Microstructural Evolution of a Silicon Oxide Phase in a Perfluorosulfonic Acid Ionomer by an *In Situ* Sol–Gel Reaction

K. A. MAURITZ,[1]* I. D. STEFANITHIS,[1] S. V. DAVIS,[1] R. W. SCHEETZ,[2] R. K. POPE,[2] GARTH L. WILKES,[3] and HAO-HSIN HUANG[3]

[1]Department of Polymer Science, University of Southern Mississippi, Hattiesburg, Mississippi 39406-0076; [2]Department of Biology, University of Southern Mississippi, Hattiesburg, Mississippi 39406-0076; [3]Department of Chemical Engineering, Virginia Polytechnic Institute and State University, Blacksburg, Virginia 24061

SYNOPSIS

Nanocomposites were produced via sol–gel reactions for tetraethylorthosilicate within the cluster morphology of perfluorosulfonic acid films. Small-angle x-ray scattering revealed that the polar/nonpolar nanophase-separated morphological template persists despite invasion by the silicon oxide phase. Scanning electron microscopy (ESEM–EDAX) studies have indicated that the greatest silicon oxide concentration occurs near the surface and decreases to a minimum in the middle. Optical and ESEM micrographs revealed a brittle, surface-attached silica layer at high silicon oxide contents. © 1995 John Wiley & Sons, Inc.

INTRODUCTION

Mauritz et al.[1–4] precipitated a highly dispersed silicon oxide phase in PFSI (PerFluoroSulfonate Ionomer, i.e. H^+ Nafion[5]) membranes via *in situ* sulfonic acid-catalyzed sol–gel reactions for tetraethoxysilane (TEOS). Water and alcohol-swollen membranes were immersed in TEOS/alcohol solutions, then dried/annealed to optimize -Si-OH group condensation. Our hypothesis was that silicon oxide phase morphology is ordered by the phase-separated morphology of Nafion consisting of clusters of polar sidechains having center-to-center spacings of around 30–50 Å.[6]

The chemical composition of the *in situ*-grown structures is represented by the formula $SiO_{2(1-¼x)}(OH)_x$ where x is considerably greater than zero, as indicated by spectroscopic studies.[1,2] Mechanical tensile studies of these hybrids revealed progressive material strengthening followed by a ductile-to-brittle transformation with increasing silicon oxide content.[1] We interpret this latter transition as reflecting inorganic phase percolation, i.e., isolated clusters become inter-knitted by a more linear-directed polycondensation and the inorganic glasslike interpenetrating network becomes the predominant load-bearing phase. FT/IR and ^{29}Si solid-state NMR spectroscopies[1,2] depicted a silicon oxide network that evolves to be increasingly less branched or less interconnected, having progressively less chain cyclization and more linearity. The view, based on mechanical tensile studies, of eventual interknitting of silicon oxide clusters, is in harmony with the notion of linear chains emerging from a cluster to intersect an adjacent cluster.

Dielectric relaxation studies[3] of these hybrids suggest cluster/matrix interfacial polarization which, in turn, suggests that clustered morphology persists after silicon oxide incorporation. The steady depression of static dielectric (real) permittivity with increasing silicon oxide uptake was rationalized in terms of progressive intergrowth of silicon oxide clusters which suppressed interfacial polarization. A DSC endotherm around 230°C for unfilled dry, H^+ Nafion was assigned to melting of crystallites consisting of TFE chains packed in hexagonal bilayers between clusters, as described by Starkweather.[7,8] This crystallinity is rather unaffected by the invasive silicon oxide, as evidenced by only minor fluctuation of the peak melting temperature of

* To whom correspondence should be addressed.

Journal of Applied Polymer Science, Vol. 55, 181–190 (1995)
 CCC 0021-8995/95/010181-10

about 230°C with increasing filler content.[4] These results reinforce our hypothesis that Nafion is a robust morphological growth template. Gas permeability vs pressure profiles for Nafion filled with silicon oxide in this way indicate dual mode sorption, which suggests the persistence of two phases.[9]

Mechanical tensile, dielectric relaxation, DSC, and gas permeation methods are only indirect probes of microstructural evolution. IR and ^{29}Si solid-state NMR spectroscopies only provide information regarding molecular groups (SiO_4, Si—O—Si, Si—OH) and their immediate environment. Knowledge of two-phase structural organization at the 10–100 Å level, presently lacking, is critical in tailoring these hybrids.

The first objective of this work was to establish, from the perspective of SAXS, whether the nano-phase-separated morphology of Nafion is a persistent template that orders the morphology of a silicon-oxide phase affected via an *in situ* sol–gel reaction for TEOS followed by drying. The second objective was to determine the distribution of silicon oxide between the surfaces of these hybrids. Presently, it is our intention to report these investigations on a qualitative level.

EXPERIMENTAL

Microcomposite Membrane Preparation

The precursor Nafion membranes used in this work were of 1100 equivalent weight and 7-mil nominal thickness.

While all membranes were received as being nominally in the acid form, we sought to ensure complete protonation of the sulfonate groups by soaking the films in 1.0 M HCl for 24 h at room temperature. Then all the membranes were removed, surface-blotted, and soaked in stirred deionized water for 24 h at 40°C in order to leach out excess HCl and affect the desired mole ratio $H^+ : SO_3^- = 1 : 1$. Therefore, the remaining intended-catalytic protons are membrane-bound and reasonably confined to the ca. 40-Å-in-size polar clusters.[6] The deionized water bath was refreshed every 8 h over this time period to promote complete free-acid extraction. Then the films were removed, blotted, and air-dried in the atmosphere for 5 h, dried under vacuum for 24 h, and finally heated at 120°C, also under vacuum.

Since Nafion exhibits swelling hysteresis and the membrane physical properties are rather sensitive to ionic form and water content, we reduced all samples to this standard initial state prior to affecting the *in situ* sol–gel reaction to maximize sample reproducibility.

All initialized membranes were equilibrated in stirred 2 : 1 (vol/vol) methanol/water solutions for 5 h at 22°C. This pre-sorbed water initiates the *in situ* sol–gel reaction given the subsequent uptake of TEOS which is introduced in quantities such that $H_2O/TEOS = 4 : 1$ (mole/mole). Solutions of 1.5 (vol/vol) TEOS/methanol were then added to the flasks that already contained the acid-form membranes in equilibrium with the above methanol/water solutions and these flasks were always stoppered after liquids were added.

The membranes were removed from these solutions after exposure to TEOS for various times. While the sol–gel reaction continues within the membranes after removal from solution, the diffusion-controlled exchange of reactants and solvent across the membrane/solution interface ceases. Therefore, the time between the addition of TEOS and the removal of the membrane from solution will be referred to as "diffusion time" rather than "reaction time." Upon removal from the solutions, the films were surface-blotted dry and finally placed under vacuum for 24 h, the last 2 h of which were spent in heating at 110°C to remove trapped volatiles and promote further silicon oxide network condensation. Dried-annealed samples were then weighed and the percent weight increase calculated.

Except for membrane initialization, the entire procedure up to the last heating step was carried out at 22°C. All samples were then stored in a desiccator prior to the SAXS and microscopy experiments.

SAXS Experiments

Small-angle X-ray scattering was carried out using an Anton–Parr Kratky camera equipped with a position-sensitive detector (PSD) from Innovative Technology, Inc. A Phillips 1729 tabletop X-ray generator with a copper target fine-focus X-ray tube was used to provide the incident X-ray radiation. The operating condition was fixed at 40 kv and 20 mA. A calibrated lupolen standard sample was used to facilitate calculation of absolute scattering intensity. The x-ray wavelength was 1.54 Å.

Microscopy

An environmental scanning electron microscope (ESEM-Electroscan E-20) was used to probe surface morphology. The x-ray energy-dispersive spectrom-

eter attachment of the ESEM (Noran System II, with ZAF correction software; spot probe set at 20 KV) was used to assess the distribution of silicon and sulfur across fields of view on surfaces and cross sections. The integrated intensity of the sulfur (S) peak in the x-ray spectrum quantifies the population of SO_3^- groups. S-peak intensity for a selected region is taken as a reference for the polymer matrix so that the Si/S intensity ratio is a relative measure of silicon oxide uptake. While microstructure at the scale of clusters is beyond ESEM resolution, the important aspect of the silicon-oxide concentration profile across the film thickness can be explored.

Pre-existing variations in polymer chemical composition (e.g., number density of SO_3H groups) and/or microstructure (e.g., crystallinity) along the thickness direction of untreated membranes might conspire to affect non-uniform inorganic concentration profiles.

Each sample was freeze-fractured after immersion in liquid nitrogen. For each of six samples, four micrographs of each freshly fractured cross section were taken of the regions: (1) "entire" cross section, i.e., including the two surfaces, at magnification of 545× for a dry, unfilled sulfonic acid membrane, and at 300× for the silicon oxide-filled samples; (2) the "central" part of the cross section (i.e., excluding near-surface regions) with magnifications from 300× to 450×; and the central part of cross sections at magnifications (3) 1000× and (4) 5000×.

For optical microscopy studies, a Nikon Optiphot optical microscope equipped with a Nikon HFX-IIA camera was used to obtain transmission micrographs of the surfaces of the six samples. For each sample, two micrographs were obtained, at 150× and 300×.

The electron and optical micrographs presented in this report were selected as representative of the large number obtained.

RESULTS AND DISCUSSION

Dry Silicon Oxide Uptake vs TEOS Diffusion Time

Percent weight uptake, relative to the initial dry acid state, for dried-annealed samples is plotted against diffusion time in Figure 1. Uptakes in this figure reach values higher than those reported earlier. For contents less than 27% the three points are co-linear in accordance with earlier-reported behavior.[1-3] However, there is accelerated uptake as content increases beyond 27%.

We suggested that the acid-catalyzed sol–gel reaction will be confined mainly to polar clusters for

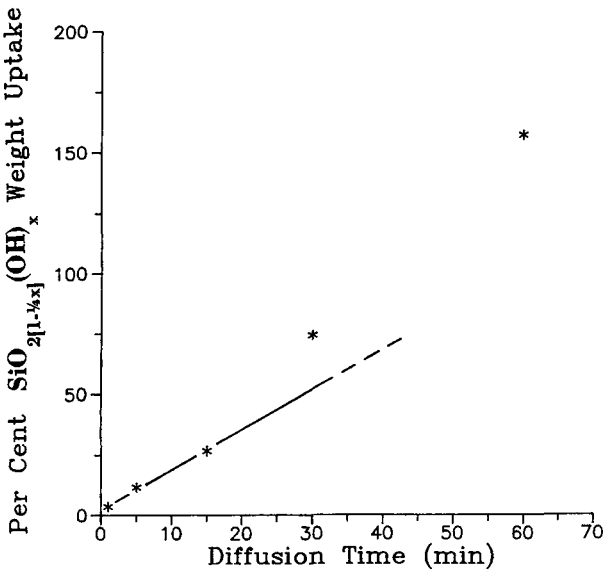

Figure 1 Percent silicon oxide dried weight uptake vs diffusion time for Nafion H^+ membranes.

short TEOS permeation times. For these low-filled systems, uptake shows linearity with time. Actually, there is a hint of upward curvature on an earlier-reported plot (Fig. 1, Ref. 4; maximum uptake 36.1%). As time increases further, the silicon oxide phase begins to percolate through the semicrystalline PFSI matrix. Eventually, silicon oxide nanoclusters become knitted together in an inorganic network which becomes the primary mechanical load-bearing component.[1]

Perhaps this accelerated uptake is due to structural change in the PFSI matrix in the form of partial disruption of chain packing within crystallites via local osmotic pressure exerted by invasive alcohol, water, TEOS, and silicic acid molecules. *Unhydrolyzed* TEOS is not highly polar, and TEOS molecules that manage to reach amorphous hydrophobic regions before hydrolysis are not incompatible with their environment. Progressive generation of more amorphous regions in this way would increase the *rate* of uptake. Melting in Nafion occurs over a broad temperature range[4,7] which implies that crystallites exist with a broad distribution of packing order and/or size. Crystallites having low T_ms might be easily disrupted upon inorganic phase incorporation. A dry SO_3H Nafion membrane of 1100 EW was cited by Fujimura et al.[10] as having a 12% weight average degree of crystallinity. Percent of crystallinity increases with annealing and may also be a function of preparative/processing conditions. The samples in this work were annealed both before and after the sol–gel reaction so that our unfilled mem-

branes might be more crystalline than 12%. Nonetheless, it is reasonable that the fraction of the matrix in the amorphous state is considerable.

WAXD is a direct monitor of crystallinity. While the preliminary SAXS investigations reported here probe structure on the higher order of nanometers, future WAXD investigations in this laboratory will address the issue of evolving crystallinity, although DSC studies[4] indicated that crystallinity of these hybrids persists at low contents. In these preliminary studies, our goal was to note qualitative trends in microstructural evolution with increasing silicon oxide uptake.

Small-Angle X-Ray Scattering

SAXS results are shown in Figure 2, in which scattering profiles are vertically shifted so that the sample with maximum content (156%) is at the bottom and there is monotonically decreasing content from bottom to top profile. Plotting shows smeared scattering intensity vs $s = 2 \sin \theta/\lambda$, θ = one-half the radial scattering angle and λ = X-ray wavelength. s^{-1} is viewed as a correlation length.

Similar to other scattering profiles reported for this system,[8,11,12] two features are seen for dry Nafion: (1) A broad peak corresponding to a long spac-

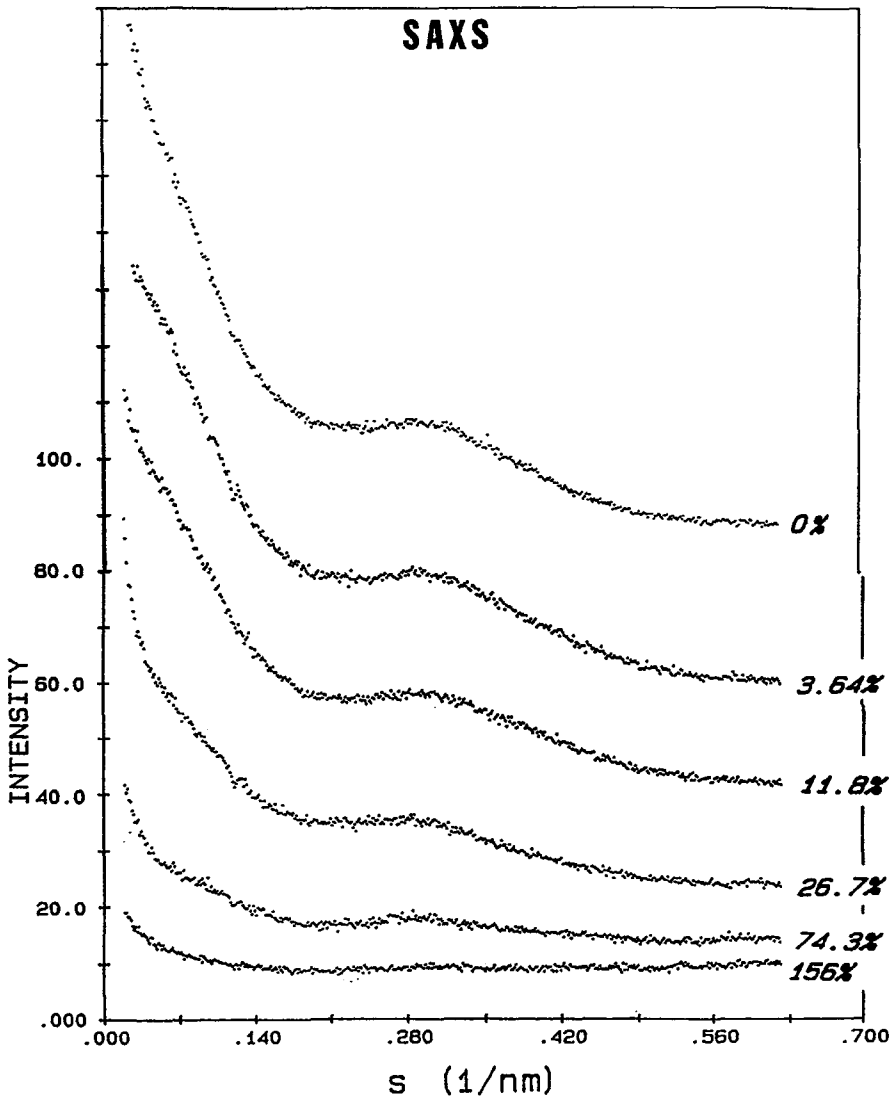

Figure 2 SAXS scattering profiles for unfilled dry H^+ 1100 EW Nafion and H^+ Nafion incorporating 3.64 to 156 wt % solid silicon oxide.

ing, ~ 3 nm, is attributed to the correlation distance caused by quasi-order within the array of polar clusters. (2) A weak shoulder in a lower-angle region ($s \sim 0.067$ nm^{-1}) corresponding to a length ~ 15 nm, is attributed to inter-crystallite spacing. A reflection observed in this latter region by Gierke et al.,[11] and similarly by Roche et al.,[13] was associated with the difference between electron densities of the crystalline and amorphous phases. Hashimoto et al.[8,10] observed a scattering maximum at $s \sim 0.07$ nm^{-1} for 1100 EW membranes, again attributed to interference of scattering by TFE crystallites.

Ding et al.,[14] reporting a SAXS study of Ni^+-neutralized sulfonated polystyrene, suggested that the region of upturn in scattered intensity near zero angle (to the left of the "ionomer peak") might be caused by effects other than crystallinity. For their system, this behavior was mentioned as being due to the neutralizing cation. Microvoids or precipitated metal salts were invoked as possible heterogeneities that might serve as scattering centers in these particular ionomers; an inhomogeneous distribution of isolated ionic groups was offered as another possibility. We are unaware of microvoid evidence in Nafion, filled or otherwise, and therefore cannot relate this concept to our near-zero-angle scattering results. The feature at $s \sim 0.07$ nm^{-1} occurs not only for different species of neutralizing counterions and H^+ form, but also for similar polymers without cations, i.e., unhydrolyzed SO_2F form as well as TFE/hexafluoropropene and TFE/perfluoropropylvinyl copolymers, as pointed out by Gierke et al.[11]

The correlation distance attributed to long-range cluster quasi-periodic spacing persists as uptake of silicon oxide increases from 0 to 156%. Even at high inorganic content, clusters persist, confirming the original hypothesis that the phase-separated morphology of Nafion is a robust interactive template for the polymerization of TEOS and subsequent morphological dispersion of the dried inorganic phase.[1-4] Presumably, tenacity of the PTFE-like crystallites as well as cluster structural cohesiveness account for this morphological persistence. This general fact is the most profound outcome of these studies. In the future, SAXS profiles will undergo mathematical analysis to extract structural details.

Brinker et al.[15] performed SAXS studies of strong acid catalyzed, sol–gel derived (TEOS) non-polymer-containing silica. It is interesting that silicate clusters with radius of gyration 15-17 Å exist in these systems. While the fact that the diameter of these clusters is approximately equal to the SAXS periodicity for unfilled Nafion membranes is fortuitous, there seems to be a natural limit to the size of a gel microparticle growing in three dimensions. Microparticles grow from their centers with decreasing density having fractal-like structures. ^{29}Si solid-state NMR and IR spectroscopic analyses of these nanocomposites depict silicon oxide chains that grow to be increasingly less interconnected[1,2] and indicate considerable Si—O—Si and O—Si—O valence bond angle distortion that becomes more severe as the gel structure grows. Inefficiency in packing accumulates during SiO_4 polymerization, leading to a network that becomes strained until discrete particle growth is impossible. In this discussion, the confining effects of the polymer matrix, especially the ubiquitous crystallites, should also be considered. In any case, we visualize that at some critical size particles cease to grow in three dimensions and sprout linear chains to intercept adjacent particles.

Scattering intensity decreases as silicon oxide content increases. Since sulfonic acid clusters have lower electron density than the surrounding regions,[8,10] the uptake of silicon oxide should reduce phase contrast, producing lower scattering intensity.

Decreasing crystallinity with increasing uptake, implied by the uptake vs time curve, is somewhat supported by the behavior of the inter-crystallite scattering feature in the very low angle region ($s \approx 0.07$ nm^{-1}). As silicon oxide content increases from 0 to 11.8%, the intensity of this shoulder decreases slightly; but as content increases to 27% and beyond, considerable decrease in intensity is observed.

Microscopy

Optical Microscopy

Optical micrographs (not shown) of dry untreated film surfaces are essentially featureless at 300×. However, surfaces of TEOS-treated samples show highly cracked patterns indicating brittle layer formation [Fig. 3(a)]. An interesting geometric relationship between cracks is that while they can curve, they always intercept each other at right angles. Thus, not all uptake is associated with *in situ* growth; rather, some uptake forms a silica layer on the surface. At 9.9% this glassy layer does not cover the entire surface, but exists in patches. As uptake increases, density and complexity of the interconnecting crack pattern increases.

Electron Microscopy

A series of parallel cracks across a glassy patch at 9.9% uptake (not shown) was probably caused by

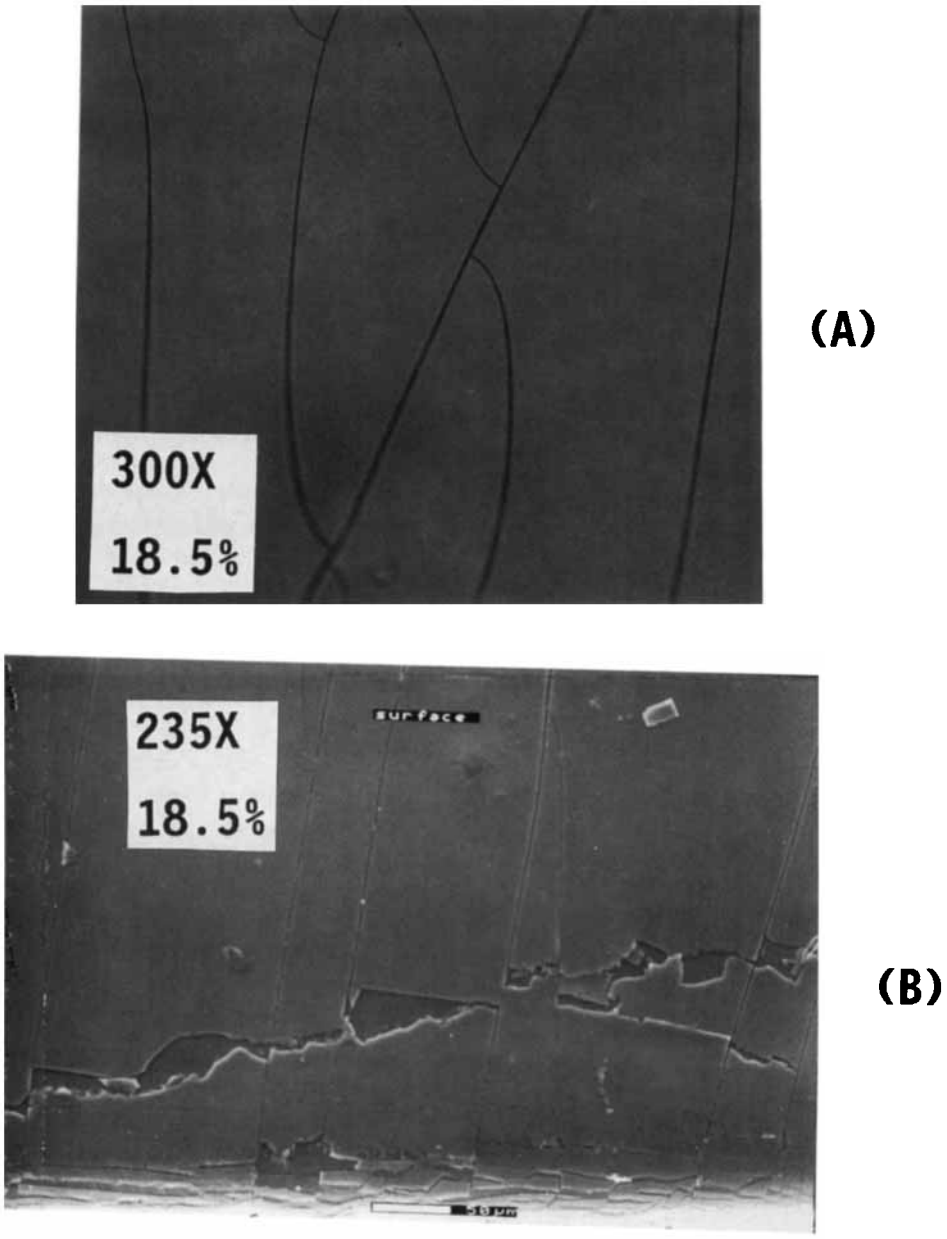

Figure 3 (a) Optical micrograph showing meeting of cracks in Nafion surface-attached silica layer (300×) for 18.5% uptake. (b) ESEM micrograph (235×) showing chipped-away regions of surfaced-attached layer for 18.5% uptake.

film bending during handling. A chipped-away layer of defined thickness is seen for 18.5% uptake [Fig. 3(b)] at 235×. In this and other figures, many cracks meet each other at 90°. It is obvious that the surface layer, around 10–30 μm thick, is brittle and can become detached in pieces. ESEM micrographs of freeze-fractured cross sections of dry unfilled H^+ Nafion at 545X [Fig. 4(a)] are essentially smooth and featureless. However, morphologies of fracture surfaces for filled samples [e.g., Fig. 4(b), 24.8% uptake @ 300×] are not smooth, having material pulled out of the cross section. Figures 4 (a) and (b) show that incorporation of silicon oxide significantly alters structural cohesiveness and ultimate mechanical strength and failure. We discussed a ductile → brittle transition for these materials which would influence fracture surface morphology. Figure 5 is a closer inspection of the middle of a cross section (9.9% @

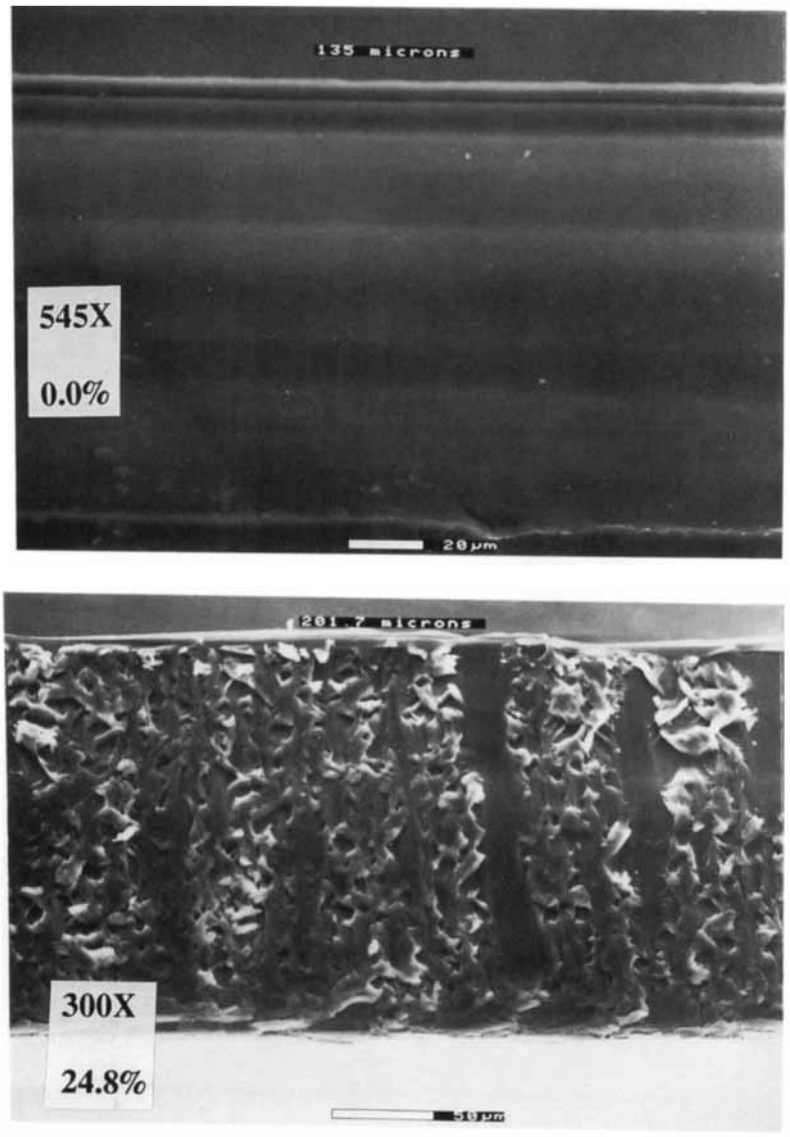

Figure 4 (a) ESEM micrograph (545×) of cross section of dry unfilled H^+ Nafion membrane. (b) ESEM micrograph (300×) of cross section of membrane with 24.8% dried silicon oxide. Both (a) and (b) are fracture surfaces.

1000×). In this and other figures, and for different uptakes, it is seen that fracture produces apparent overlapping material layers with curved edges. At 5000× the overlapping feature is not as distinct and the morphology becomes more featureless.

From ESEM micrographs, we determined film thickness vs uptake (Fig. 6) to see whether mass increases (a) isotropically or (b) by one-dimensional growth normal to film surfaces by silicon oxide incorporation on surfaces or in near-surface regions. Thickness in (a) is proportional to $(\text{mass})^{1/3}$, whereas in (b) it is directly proportional to mass. The curve approaches linearity and increase in thickness over the linear section in approximately the inorganic layer thickness observed in micrographs. Prior to linearity the curve is concave downward, although not enough points are available to test for a $(\text{mass})^{1/3}$ relationship. It will follow, from the discussion below of Si distribution across the thickness, that isotropic expansion is unreasonable.

Distribution of Silicon Oxide

Figure 7 shows plots of Si/S intensity ratio vs uptake for (a) an entire cross section, and (b) the corre-

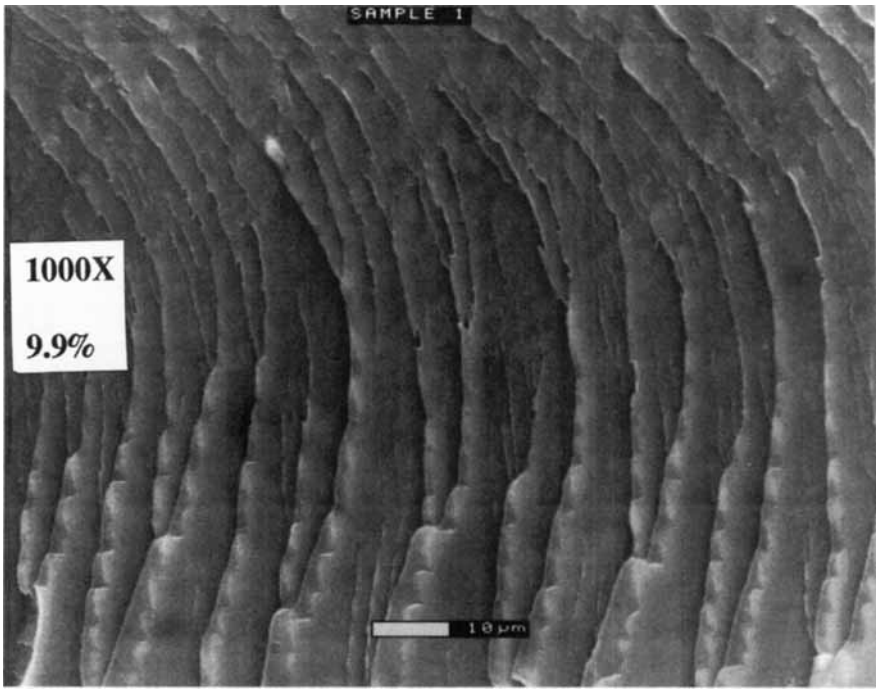

Figure 5 ESEM micrograph (1000×) of cross section fracture surface for 9.9% silicon oxide.

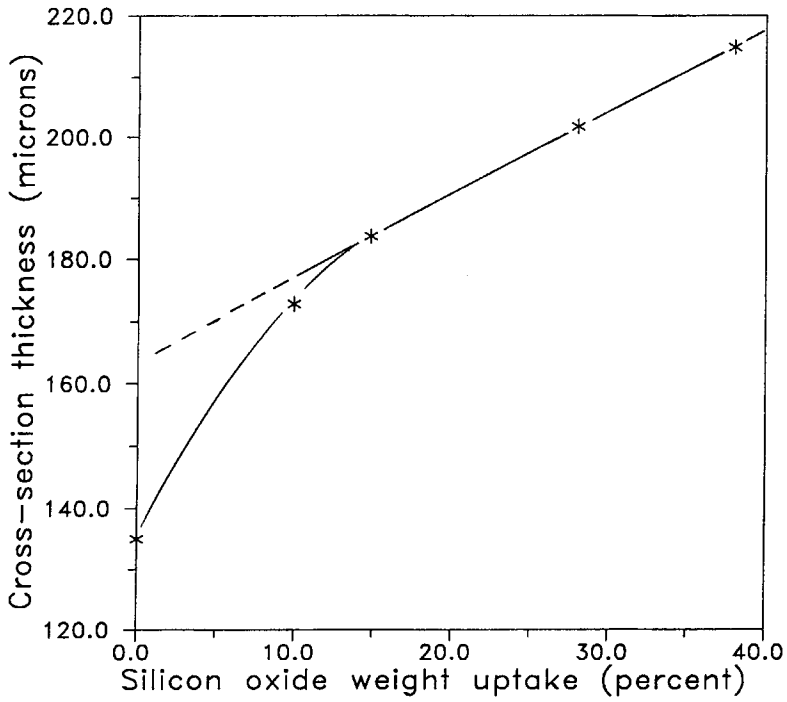

Figure 6 Thickness (from ESEM) vs dried silicon oxide uptake of H^+ Nafion films.

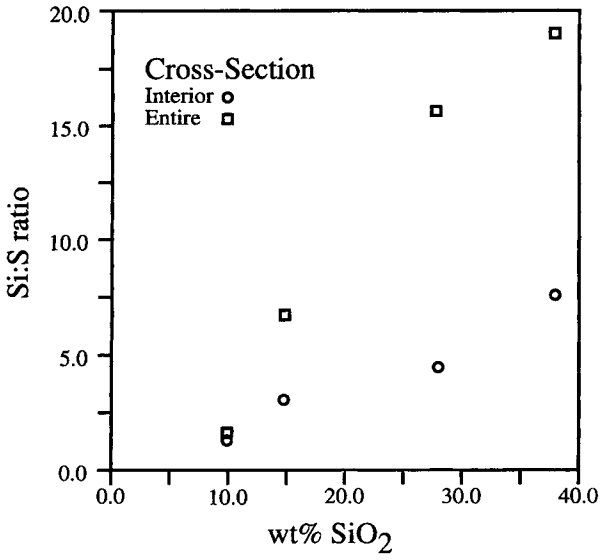

Figure 7 Si/S x-ray peak intensity ratio vs silicon oxide content for an entire (upper) and interior (lower) nanocomposite cross section.

sponding interior area (i.e., 5000 nm thick region); both increase monotonically. There is significantly more Si in the near-surface than interior regions and Si/S seems to increase at a greater rate in near-surface regions. Recall that optical and ESEM micrographs of exterior surfaces revealed brittle surface-attached layers. These contiguous (although cracked) layers are silica-like and contain no polymeric material. Pure Nafion is rather extensible and does not fracture at this temperature.

We also performed point-by-point spot mode analyses of Si/S across the thickness, each point reflecting relative composition within a small area. Sample results are in Figure 8 for two uptakes; the same general distribution exists for other uptakes. For each graph, one surface is positioned at the left on the vertical axis and the other surface position is indicated to the right. The difference in right positions reflects different filler contents. The curves rise overall with increased uptake. Silicon oxide concentration decreases proceeding inward from either near-surface and is minimum in the middle. The horizontal dashed lines represent overall (surface + interior), or average Si/S ratio.

CONCLUSIONS

Our first objective was to establish whether the nanophase-separated morphology of Nafion is in fact a template for the morphology of a silicon-oxide phase incorporated via *in situ* sol–gel reactions for TEOS. The fact that the SAXS peak, identified with quasi-order among clusters in unfilled Nafion, persists when these systems are filled with silicon oxide suggests that this objective has been achieved. In the future, visual evidence via high-resolution microscopy will be obtained. The decrease in SAXS peak intensity with increasing silicon-oxide content

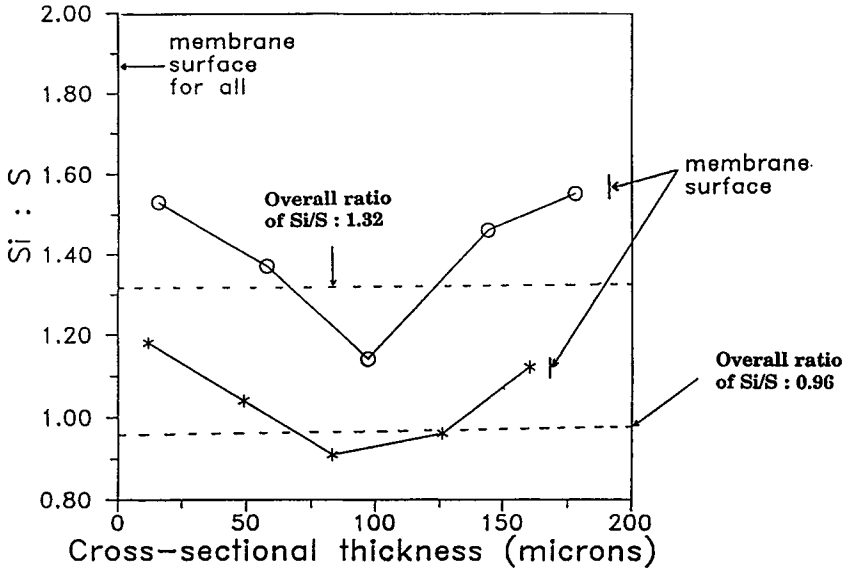

Figure 8 Si/S x-ray peak intensity ratio distribution across thickness of nanocomposites with indicated overall Si/S ratios.

is believed to reflect reduction in electron-density contrast between cluster and matrix phases.

Our second objective was to achieve qualitative understanding of silicon-oxide distribution between the membrane surfaces. ESEM studies indicated that the greatest concentration occurs at the near-surface and decreases to a minimum in the middle. Consequently, silicon-oxide phase percolation must occur throughout near-surface regions before it does in the middle. It would seem that the nonhomogeneous distribution of silicon oxide would influence the SAXS peak, although the peak position is rather invariant with uptake.

It is imagined that mechanical, electrical, dielectric, optical, and diffusion property gradients might be tailored to optimize these systems for various applications.

Both optical and electron micrographs revealed a brittle, surface-attached silica layer at high silicon-oxide contents, though not at low contents.

Silicon oxide distribution is controlled by a complexity of factors, including diffusion rates of $Si(OR)_x(OH)_{4-x}$ molecules, sol–gel reaction rates, and accumulation of gel at a given place and time. Thus it would seem that with gel structure initiating in near-surface regions, later-sorbed $Si(OR)_x(OH)_{4-x}$ molecules encounter progressively more obstacles in diffusion to the middle plane of the film. Ultimately, with diffusion pathways blocked, pure silica would be forced to precipitate on the surface. These layers are undesirable from an applications standpoint and studies are in progress to determine whether surface precipitation can be inhibited by ion-exchanging the membrane from the H^+ to various cation forms.

[Organic]/[inorganic oxide] nanocomposite membranes have potential applications in the arenas of industrial gas separations, chlor-alkali and fuel cells, dielectrics, nonlinear optics, and heterogeneous catalysis technologies.

Acknowledgment is made to the donors of the Petroleum Research Fund, administered by the American Chemical Society, for support of this research. We are also thankful to E. I. DuPont de Nemours & Co. for their donation of Nafion 117 membranes.

REFERENCES

1. K. A. Mauritz, R. F. Storey, and C. K. Jones, in *Multiphase Polymer Materials: Blends, Ionomers, and Interpenetrating Networks,* L. A. Utracki and R. A. Weiss, Eds., ACS Symp. Ser. No. 395, Amer. Chem. Soc., Washington, DC, 1989.
2. K. A. Mauritz and R. M. Warren, *Macromolecules,* **22,** 1730 (1989).
3. K. A. Mauritz and I. D. Stefanithis, *Macromolecules,* **23,** 1380 (1990).
4. I. D. Stefanithis and K. A. Mauritz, *Macromolecules,* **23,** 2397 (1990).
5. *Nafion* is a registered trademark of E. I. DuPont de Nemours and Co., Inc.
6. K. A. Mauritz, *J. Macromol. Sci. Rev. Macromol. Chem. Phys.,* **C28**(1), 65 (1988).
7. H. W. Starkweather, Jr., *Macromolecules,* **15,** 320 (1982).
8. T. Hashimoto, M. Fujimura, and H. Kawai, in *Perfluorinated Ionomer Membranes,* ACS Symp. Ser. 180, A. Eisenberg and H. L. Yeager, Eds., Amer. Chem. Soc., Washington, DC, 1982.
9. S. V. Davis and K. A. Mauritz, *Am. Chem. Soc. Polymer Preprints,* **33**(2), 363 (1992).
10. M. Fujimura, T. Hashimoto, and H. Kawai, *Macromolecules,* **14,** 1309 (1981).
11. T. D. Gierke, G. E. Munn, and F. C. Wilson, *J. Polym. Sci., Polym. Phys. Ed.,* **19,** 1687 (1981).
12. R. B. Moore and C. R. Martin, *Macromolecules,* **21,** 1334 (1988).
13. E. J. Roche, M. Pineiri, R. Duplessix, and A. M. Levelut, *J. Polym. Sci., Polym. Phys. Ed.,* **19,** 1 (1981).
14. Y. S. Ding, S. R. Hubbard, K. O. Hodgson, R. A. Register, and S. L. Cooper, *Macromolecules,* **21,** 1698 (1988).
15. C. J. Brinker, K. D. Keefer, D. W. Schaefer, and C. S. Ashley, *J. Non-Crystalline Solids,* **48,** 47 (1982).

Received March 25, 1994
Accepted July 1, 1994